Response discontinuities in the solution of the incremental Mori–Tanaka scheme for elasto-plastic composites

P. SADOWSKI*, K. KOWALCZYK-GAJEWSKA, S. STUPKIEWICZ

*Institute of Fundamental Technological Research,
Polish Academy of Sciences,
Pawińskiego 5B, 02–106 Warsaw, Poland
e-mails: psad@ippt.pan.pl, kkowalcz@ippt.pan.pl, sstupkie@ippt.pan.pl*

The incremental Mori–Tanaka model of elasto-plastic composites is discussed, and the corresponding finite-step formulation is shown to lead to discontinuities in the overall response at the instant of elastic-to-plastic transition in the matrix. Specifically, two situations may be encountered: the incremental equations may have two solutions or no solution. In the former situation, switching between the two solutions is associated with a jump in the overall stress. Response discontinuities are studied in detail for a special case of proportional deviatoric loading. The discontinuities constitute an undesirable feature of the incremental Mori–Tanaka scheme that apparently has not been discussed in the literature so far. Remedies to the related problems are briefly discussed.

Key words: mean-field homogenization, Mori–Tanaka method, incremental scheme, composite materials, elasto-plasticity.

1. Introduction

MEAN-FIELD HOMOGENIZATION METHODS, such as the Mori–Tanaka method [1, 2], self-consistent and generalized self-consistent method [3–6], differential and incremental schemes [7, 8] or double- and coated-inclusion methods [9, 10], offer good predictive capabilities at low computational cost, as compared to much more involved multiscale methods, such as the FE^2 method [11, 12].

Since those methods were originally developed for elastic composites, their application in the context of non-linear material behavior requires proper linearization of the governing stress–strain relations. Different approaches have been proposed in the literature, namely the transformation field analysis with elastic localization rule and inelastic strain playing the role of eigenstrain [13], incremental tangent [4, 14], secant [15], non-incremental tangent [16–19], asymptotic tangent [20], additive tangent [21] or sequential [22] linearization procedures.

Among the mean-field approaches mentioned above, the Mori–Tanaka (MT) scheme, due to its simplicity, seems to be the most often used method applied to

---

*Corresponding author.

metal-matrix composites covering a large range of material behaviours, including elasto-plasticity [13, 23, 24], elasto-viscoplasticity [15, 25, 26], damage [20, 27], phase transformations [28, 29], shape memory effects [30–32], and others. Extensions to the finite strain regime have also been reported [33, 34].

This paper is focused on the incremental MT scheme applied to elasto-plastic composites. The scheme has been originally formulated in the rate form that employs the instantaneous tangent moduli [4, 35] of the matrix phase. Its practical application, for instance, in the finite element method, requires time integration of the rate equations, and a robust implementation of an incremental finite-step model is essential.

The incremental MT scheme is based on the Eshelby concept of an inclusion immersed in an infinite matrix [36]. Accordingly, the Eshelby tensor (or the polarization tensor) that depends on the tangent stiffness tensor of the matrix is needed. The elasto-plastic tangent tensor is in general anisotropic so that the corresponding Eshelby tensor (or the polarization tensor) would have to be calculated employing numerical integration. However, isotropization of the elasto-plastic tangent is usually performed in order to avoid an overly stiff response [23, 24], and closed-form formulae are available for an isotropic stiffness tensor. Note that isotropization is not always needed, e.g., when the so-called additive tangent MT scheme is applied to elasto-viscoplastic composites [26].

Early finite element implementations of the incremental MT scheme go back to the works of Pettermann et al. [35] and Doghri and Ouaar [23]; in [35], the temperature effects were additionally taken into account. In those models, micro-macro transition relations were obtained via strain concentration tensors expressed in terms of the algorithmic (consistent) tangent stiffness tensor of the matrix, and an implicit iterative scheme was employed to solve the resulting nonlinear equations. Consistent linearization of the overall response was not attempted, hence quadratic convergence could not be achieved at the global level. Computational schemes capable of consistent linearization of the overall response have been developed, e.g., in [37, 38].

A formulation suitable for automation and leading to an efficient and robust incremental MT model has been recently developed by Sadowski et al. [39]. Accordingly, relatively large load (strain) increments have been employed in finite element computations, and the simulations have revealed convergence problems that turn out to be related to discontinuities in the incremental finite-step response. Those discontinuities are discussed in the present paper.

Detailed analysis is carried out for a special case of proportional deviatoric loading in which the governing equations reduce to scalar (rather than tensorial) equations. The analysis shows that two situations may be encountered depending on the properties of the phases and on the details of the formulation of the incremental MT method. It is shown that a range of overall strain increments

exists in which the incremental equations have two solutions or no solution at all. Furthermore, if there are two solutions, then the overall stresses corresponding to those solutions differ one from the other, and switching between the two solutions is associated with a jump in the overall stress.

Apparently, the response discontinuities and the related features of the incremental MT method have not been discussed in the literature so far.

2. The Mori–Tanaka homogenization approach

2.1. Micro- and macro-response of elastic composite

The Mori–Tanaka scheme [1] is a mean-field model originally dedicated to the estimation of effective properties of linearly elastic two-phase composites. It originates from the Eshelby solution to the problem of an ellipsoidal inclusion embedded into an infinite linearly elastic matrix [36]. The main outcome of this solution is that the strain inside the inclusion ε_1 is uniform and related to the far-field strain ε_0 in the matrix by the fourth-order Eshelby tensor. Hill [4] noticed an important consequence of this result that has been written in the form of the so-called *interaction equation*,

$$(2.1) \qquad \boldsymbol{\sigma}_1 - \boldsymbol{\sigma}_0 = -\mathbb{L}_* \left(\boldsymbol{\varepsilon}_1 - \boldsymbol{\varepsilon}_0 \right),$$

where $\boldsymbol{\sigma}_1$ and $\boldsymbol{\sigma}_0$ denote the stress tensor in the inclusion and the far-field stress tensor, respectively. $\mathbb{L}_*$ is the fourth-order tensor, called the Hill tensor, which can be expressed in terms of the polarization tensor $\mathbb{P}$,

$$(2.2) \qquad \mathbb{L}_* = \mathbb{P}^{-1} - \mathbb{L}_0, \qquad \mathbb{P} = \hat{\mathbb{P}}(\mathbb{L}_0),$$

and $\mathbb{P}$ depends only on the elastic stiffness $\mathbb{L}_0$ of the matrix and on the shape of inclusions [40]. Here the superimposed hat is used to distinguish the function from its value.

Now, let us consider a two-phase composite material composed of ellipsoidal inclusions embedded in a matrix. The MT model is obtained by identifying ε_0 and $\boldsymbol{\sigma}_0$ with the average strain and stress in the matrix, respectively. Furthermore, the matrix is identified as the reference medium in the interaction equation (2.1), so that the Hill tensor $\mathbb{L}_*$ is evaluated in terms of the elastic stiffness $\mathbb{L}_0$ of the matrix, as in Eq. (2.2).

The overall strain and stress in the two-phase composite are obtained by averaging of the corresponding local quantities,

$$(2.3) \qquad \bar{\varepsilon} = (1 - c)\,\varepsilon_0 + c\varepsilon_1, \qquad \bar{\boldsymbol{\sigma}} = (1 - c)\,\boldsymbol{\sigma}_0 + c\boldsymbol{\sigma}_1,$$

where c is the volume fraction of inclusions. The overall response of the elastic composite can now be obtained from the interaction equation (2.1) and the

averaging rule (2.3), using also the linear constitutive equations of the individual phases, $\boldsymbol{\sigma}_i = \mathbb{L}_i \boldsymbol{\varepsilon}_i$, $i = 0, 1$.

2.2. Incremental Mori–Tanaka scheme

The MT scheme, originally formulated for elastic composites, can be adapted to elasto-plastic composites by applying incremental linearization, as proposed by Hill [4]. Within that scheme, linearization of the non-linear behavior of the phases is performed, and the rate form of the constitutive equation of the i-th phase is used for that purpose,

$$(2.4) \qquad\qquad \dot{\boldsymbol{\sigma}}_i = \mathbb{L}_i^{\mathrm{ep}} \dot{\boldsymbol{\varepsilon}}_i \,,$$

where $\mathbb{L}_i^{\mathrm{ep}}$ is the current elasto-plastic (constitutive) tangent stiffness tensor of the respective phase. The interaction equation takes the following rate form:

$$(2.5) \qquad\qquad \dot{\boldsymbol{\sigma}}_1 - \dot{\boldsymbol{\sigma}}_0 = -\mathbb{L}_* \left(\dot{\boldsymbol{\varepsilon}}_1 - \dot{\boldsymbol{\varepsilon}}_0 \right),$$

where the Hill tensor $\mathbb{L}_*$:

$$(2.6) \qquad\qquad \mathbb{L}_* = \mathbb{P}^{-1} - \mathbb{L}_0^{\mathrm{ep}}, \qquad \mathbb{P} = \hat{\mathbb{P}}(\mathbb{L}_0^{\mathrm{ep}}),$$

and the polarization tensor $\mathbb{P}$ depends now on the elasto-plastic tangent $\mathbb{L}_0^{\mathrm{ep}}$ and, as in the elastic case, on the inclusion shape. Note that the elasto-plastic tangent $\mathbb{L}_0^{\mathrm{ep}}$ is anisotropic even if the material itself is isotropic, and various isotropization schemes are usually applied to avoid an excessively stiff overall response [23, 24], see Appendix B.

Using Eq. (2.4), the interaction equation (2.5) can be written in the following equivalent form:

$$(2.7) \qquad\qquad \dot{\boldsymbol{\varepsilon}}_1 = \left(\mathbb{I} + \mathbb{P}(\mathbb{L}_1^{\mathrm{ep}} - \mathbb{L}_0^{\mathrm{ep}}) \right)^{-1} \dot{\boldsymbol{\varepsilon}}_0.$$

As in the case of an elastic composite, the overall rate response of the elasto-plastic composite is then obtained by solving the interaction equation (2.7) and the averaging rule (2.3).

2.3. Incremental finite-step formulation

The theory presented in the preceding subsections is nowadays well established. In order to use the incremental MT method in practice, e.g., as a two-phase material model in the framework of the finite element method, the rate equations in Section 2.2 must be integrated over time. Application of a time integration scheme leads to an incremental finite-step formulation in which, at

a typical time step $t_n \to t_{n+1}$, the quantities at t_n are known, and the current quantities at t_{n+1} are to be found by solving the incremental problem.

By applying a generalized mid-point rule [23] to the linearized constitutive equation (2.4), the following finite-step relationship is obtained:

$$(2.8) \qquad \Delta\boldsymbol{\sigma}_i = \mathbb{L}_i^{\mathrm{ep},n+\theta}\Delta\boldsymbol{\varepsilon}_i, \qquad \mathbb{L}_i^{\mathrm{ep},n+\theta} = (1-\theta)\mathbb{L}_i^{\mathrm{ep},n} + \theta\mathbb{L}_i^{\mathrm{ep},n+1},$$

where $\theta \in [0,1]$, the superscript n or $n+1$ indicates the time instant at which the quantity is evaluated, and Δ denotes the increment, so that, for instance, $\Delta\boldsymbol{\varepsilon}_i = \boldsymbol{\varepsilon}_i^{n+1} - \boldsymbol{\varepsilon}_i^n$. The interaction equation (2.5) is also expressed in terms of increments,

$$(2.9) \qquad\qquad \Delta\boldsymbol{\sigma}_1 - \Delta\boldsymbol{\sigma}_0 = -\mathbb{L}_*\left(\Delta\boldsymbol{\varepsilon}_1 - \Delta\boldsymbol{\varepsilon}_0\right),$$

where the Hill tensor $\mathbb{L}_*$ depends now on the tangent operator $\mathbb{L}_0^{\mathrm{ep},n+\theta}$,

$$(2.10) \qquad\qquad \mathbb{L}_* = \mathbb{P}^{-1} - \mathbb{L}_0^{\mathrm{ep},n+\theta}, \qquad \mathbb{P} = \hat{\mathbb{P}}(\mathbb{L}_0^{\mathrm{ep},n+\theta}).$$

The averaging rule (2.3) completes the set of governing equations from which the overall stress increment $\Delta\bar{\boldsymbol{\sigma}}$ can be computed for a prescribed overall strain increment $\Delta\bar{\boldsymbol{\varepsilon}}$. Note that, unlike in the rate formulation in Section 2.2, the interaction equation (2.9) in the finite-step formulation is *not* equivalent to the finite-step counterpart of Eq. (2.7), viz.

$$(2.11) \qquad\qquad \Delta\boldsymbol{\varepsilon}_1 = \left(\mathbb{I} + \mathbb{P}(\mathbb{L}_1^{\mathrm{ep},n+\theta} - \mathbb{L}_0^{\mathrm{ep},n+\theta})\right)^{-1}\Delta\boldsymbol{\varepsilon}_0,$$

because the latter explicitly exploits the linearized constitutive equations (2.8), while the former does not. In fact, the actual stress increments $\Delta\boldsymbol{\sigma}_i = \boldsymbol{\sigma}_i^{n+1} - \boldsymbol{\sigma}_i^n$ can be employed in the interaction equation (2.9) instead of the approximate increments resulting from the linearization (2.8), and this formulation is adopted in the present work, see also [26, 39]. Formulations based on Eq. (2.11) are employed, e.g., in [23, 35, 38].

The governing equations of the incremental MT scheme are non-linear and thus must be solved iteratively, e.g., using the Newton method. The solution must then be linearized in order to compute the overall consistent (algorithmic) tangent $\bar{\mathbb{L}}^{\mathrm{alg}} = \partial\Delta\bar{\boldsymbol{\sigma}}/\partial\Delta\bar{\boldsymbol{\varepsilon}}$ which is needed, for instance, when the MT model is used as a constitutive model in FE computations. Consistent linearization of the resulting doubly-nested iteration-subiteration scheme, which is not a trivial task, and its impact on the overall performance of the elasto-plastic MT model are discussed in detail by Sadowski *et al.* [39].

Let us note that exact linearization of the incremental MT model is usually not performed in practical applications of the incremental MT scheme,

e.g., [23, 35]. Actually, the fixed point iteration method, used in [23, 35] to solve the incremental equations resulting from the MT scheme, does not admit exact linearization. Problems with exact linearization of the elasto-plastic MT model have been mentioned also in other related papers, e.g., [29, 41]. As an exception, a computational scheme that includes exact linearization of the MT model has been reported in [37, 38].

Let us note also that in some formulations, e.g. [23, 35, 39, 41], the incremental linearization (2.8) and the corresponding interaction equation (2.9) employ the algorithmic tangent $\mathbb{L}_i^{\mathrm{alg}} = \partial\Delta\boldsymbol{\sigma}_i/\partial\Delta\boldsymbol{\varepsilon}_i$ rather than the constitutive elasto-plastic tangent $\mathbb{L}_i^{\mathrm{ep}}$.

As explained above, incremental linearization of the constitutive equations is an essential element of the elasto-plastic MT scheme. In case of rate equations, linearization (2.4) is exact, even though the elasto-plastic tangent $\mathbb{L}_0^{\mathrm{ep}}$ suffers discontinuity at the transition from the elastic to the plastic state. The discontinuity of the local tangent results then in discontinuity of the overall tangent, but the overall response is continuous.

However, for a finite step, linearization (2.8) provides only an approximation of the actual incremental response. Moreover, if the step involves the elastic-to-plastic transition, then the accuracy of the approximation delivered by the current (weighted) elasto-plastic tangent may be low. This may lead to response discontinuities that constitute the main concern of the present paper and apparently have not been discussed in the literature yet.

3. Response discontinuities for proportional deviatoric loading

3.1. Origin of response discontinuities at the elastic-to-plastic transition

Consider the finite-step incremental MT scheme introduced in Section 2.3 and a time increment that would correspond to the elastic-to-plastic transition in the matrix. The matrix is thus assumed to be in an elastic state at $t = t_n$. Furthermore, we introduce a parametrization of the overall strain increment $\Delta\bar{\boldsymbol{\varepsilon}} = \alpha\boldsymbol{\epsilon}$, with $\alpha > 0$ and $\boldsymbol{\epsilon}$ fixed, such that for small α the matrix is still elastic, but for sufficiently large α it would be plastic at $t = t_{n+1}$.

Now, we observe that the tangent operator $\mathbb{L}_0^{\mathrm{ep},n+1}$ and thus also $\mathbb{L}_0^{\mathrm{ep},n+\theta}$ suffer discontinuity at the instant of elastic-to-plastic transition. Actually, for $\theta = 0$ the latter one would not change with an increasing α, but the corresponding explicit Euler scheme is highly inaccurate, and is thus not considered here. Typical values for θ are $\theta = 0.5$ (mid-point rule) and $\theta = 1$ (backward Euler scheme).

Discontinuity of $\mathbb{L}_0^{\mathrm{ep},n+\theta}$ implies discontinuity of the Hill tensor $\mathbb{L}_*$ in the interaction equation (2.9) and this results in discontinuity of the solution of the

equations governing the incremental MT scheme. As a result, the overall stress may suffer discontinuity at the instant of elastic-to-plastic transition. Actually, as shown below, a range of values of the scaling parameter α can be found for which either there is no solution or there are two solutions, each associated with a different value of the overall stress. The two situations are schematically illustrated in Fig. 2 that is discussed in detail in Section 3.5.

Considering application of the incremental MT model in finite element computations, the two situations mentioned above are highly undesirable since they negatively affect the convergence properties and overall robustness of the corresponding finite element scheme.

The related convergence problems are illustrated in Fig. 1a that shows, after [39], the results of finite element computations in which the incremental MT scheme has been used as the constitutive model evaluated at the Gauss points. The results correspond to tension of a rectangular plate with a central hole. The material was a two-phase composite with an elasto-plastic matrix and spherical elastic inclusions. The finite element model involved 368 640 hexahedral elements and about 1.2 million degrees of freedom. More details can be found in [39].

The response discontinuities discussed above were frequently encountered during the solution process, and the computations could only proceed with rather small load increments, see Fig. 1a. For larger load increments, convergence of the
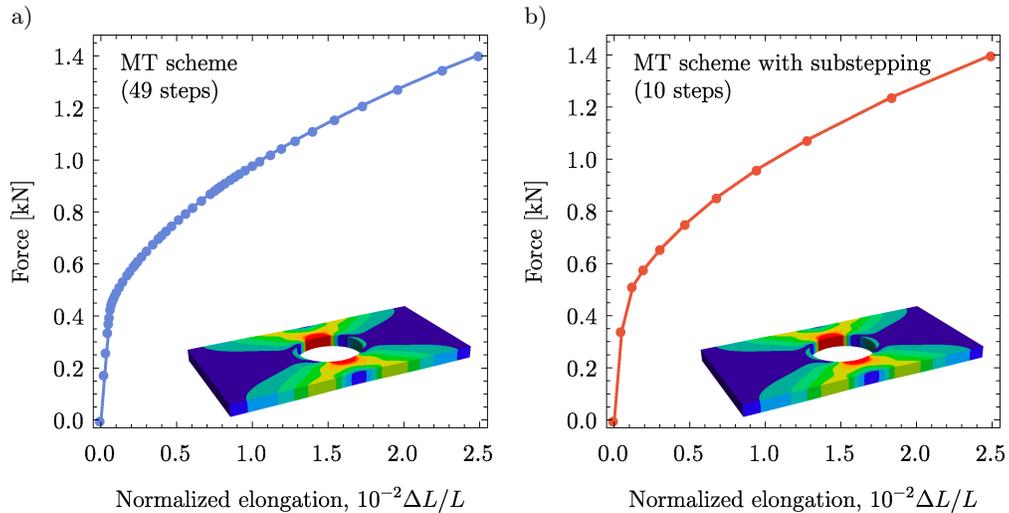
Fig. 1. Illustration of the impact of response discontinuities on the convergence behavior and robustness of the incremental MT scheme employed in finite element computations: a) basic MT scheme exhibiting severe convergence problems that are caused by the discontinuities; b) MT scheme enhanced by a substepping strategy that eliminates the discontinuities. The diagrams present the force–displacement curves with dots indicating the load steps for the problem of tension of a rectangular composite block with a hole, cf. [39].

global Newton iterations could not be achieved. On the other hand, as shown in Fig. 1b, the solution could be obtained in just 10 large steps once the MT scheme has been combined with a substepping strategy that eliminates the response discontinuities, cf. Section 4. The enhanced incremental MT scheme proves therefore to be highly robust and thus suitable for large-scale simulations.

Below, the response discontinuities are studied in detail for a special case of proportional deviatoric loading for which the incremental solution can be found in a closed form. Some remedies are discussed next.

3.2. Proportional deviatoric loading

From now on, the discussion is restricted to a two-phase composite with spherical isotropic elastic inclusions, uniformly dispersed in an elasto-plastic isotropic matrix that obeys the J_2-plasticity model with linear isotropic hardening.

A strain-controlled, proportional loading is considered so that the overall strain $\bar{\varepsilon}$ can be expressed as

$$(3.1) \qquad \bar{\varepsilon} = \bar{\varepsilon}\mathbf{N},$$

where $\bar{\varepsilon}$ increases monotonically, and $\mathbf{N}$ is a constant tensor satisfying the following conditions

$$(3.2) \qquad \mathbf{N} = \text{const}, \qquad \text{tr}\,\mathbf{N} = 0, \qquad \|\mathbf{N}\| = 1.$$

Accordingly, the overall strain $\bar{\varepsilon}$ is a deviator, $\text{tr}\bar{\varepsilon} = 0$, and so is its increment $\Delta\bar{\varepsilon}$,

$$(3.3) \qquad \Delta\bar{\varepsilon} = \Delta\bar{\varepsilon}\mathbf{N}.$$

The incremental MT scheme is now employed based on the interaction equation (2.9) in which the elasto-plastic tangent $\mathbb{L}_0^{\text{ep},n+1}$ is used to compute the Hill tensor $\mathbb{L}_*$ and the polarization tensor $\mathbb{P}$, i.e., the backward Euler scheme ($\theta = 1$) is applied. Furthermore, following the usual practice, the polarization tensor $\mathbb{P}$ is evaluated in terms of the isotropized tangent, see Appendix B. Other options are discussed in Sections 3.7 and 4. It is shown, see Appendix A, that under those assumptions all local and total stress and strain tensors are also proportional to $\mathbf{N}$, namely

$$(3.4) \qquad \Delta\bar{\boldsymbol{\sigma}} = \Delta\bar{\sigma}\mathbf{N}, \qquad \Delta\boldsymbol{\varepsilon}_i = \Delta\varepsilon_i\mathbf{N}, \qquad \Delta\boldsymbol{\sigma}_i = \Delta\sigma_i\mathbf{N} \qquad \text{for } i = 0, 1,$$

and the problem can be treated as one-dimensional. As a consequence, equations introduced in Section 2 can be written in a scalar form.

The incremental interaction equation (2.9) is thus written as follows:

$$(3.5) \qquad \Delta\sigma_1 - \Delta\sigma_0 = -2G_*^{\text{ep}} \left(\Delta\varepsilon_1 - \Delta\varepsilon_0 \right),$$

where

$$(3.6) \qquad G_*^{\mathrm{ep}} = \frac{1}{2P^{\mathrm{ep}}} - G_0^{\mathrm{ep}}, \qquad P^{\mathrm{ep}} = \frac{3(2G_0^{\mathrm{ep}} + K_0^{\mathrm{e}})}{5G_0^{\mathrm{ep}}(4G_0^{\mathrm{ep}} + 3K_0^{\mathrm{e}})},$$

and K_0^{e} is the elastic bulk modulus of the matrix. Here, G_*^{ep} and P^{ep} are scalar coefficients derived from the respective tensors $\mathbb{L}_*$ and $\mathbb{P}$, see Appendix A, and $\mathbb{P}$ is determined using the isotropized tangent shear modulus $G_0^{\mathrm{ep(iso)}}$ specified by Eq. (B.1), so that $G_0^{\mathrm{ep(iso)}} = G_0^{\mathrm{ep}}$, compare Eqs. (A.10) and (B.1). Superscript 'ep' refers to the quantities associated with the general constitutive elasto-plastic tangent. Superscripts 'e' or 'p' refer to the quantities related, respectively, to the elastic or plastic state of the matrix.

The incremental form of the averaging rule is now the following:

$$(3.7) \qquad \Delta\bar{\varepsilon} = (1 - c)\Delta\varepsilon_0 + c\Delta\varepsilon_1, \qquad \Delta\bar{\sigma} = (1 - c)\Delta\sigma_0 + c\Delta\sigma_1.$$

The incremental constitutive equations take the form

$$(3.8) \qquad \Delta\sigma_0 = 2G_0^{\mathrm{e}}(\Delta\varepsilon_0 - \Delta\gamma_0), \qquad \Delta\sigma_1 = 2G_1^{\mathrm{e}}\Delta\varepsilon_1,$$

where G_0^{e} and G_1^{e} are the elastic shear moduli of the matrix and the inclusions, respectively. The matrix may undergo plastic deformation, thus Eq. $(3.8)_1$ includes the increment of plastic multiplier $\Delta\gamma_0 \geq 0$. The yield function of the matrix can also be written in a scalar form,

$$(3.9) \qquad \phi_0^{n+1} = \sigma_0^n + \Delta\sigma_0 - \sigma_{\mathrm{y},0} - H_0(\gamma_0^n + \Delta\gamma_0),$$

where $\sigma_{\mathrm{y},0}$ is the initial yield stress, H_0 is the hardening modulus, and the following standard complementarity conditions hold:

$$(3.10) \qquad \Delta\gamma_0 \geq 0, \qquad \phi_0^{n+1} \leq 0, \qquad \Delta\gamma_0\,\phi_0^{n+1} = 0.$$

3.3. Elastic step

First, a fully elastic step is considered so that $\phi_0^{n+1} \leq 0$, $\Delta\gamma_0 = 0$ and $G_0^{\mathrm{ep}} = G_0^{\mathrm{e}}$. Solution of Eqs. (3.5)–(3.9) yields the following elastic response

$$(3.11) \qquad \Delta\sigma_0 = 2G_0^{\mathrm{e}}\Delta\varepsilon_0, \quad \Delta\sigma_1 = 2G_1^{\mathrm{e}}\Delta\varepsilon_1, \quad \Delta\varepsilon_0 = \alpha_0^{\mathrm{e}}\Delta\bar{\varepsilon}, \quad \Delta\varepsilon_1 = \alpha_1^{\mathrm{e}}\Delta\varepsilon_0,$$

and

$$(3.12) \qquad \Delta\bar{\sigma} = 2\alpha_0^{\mathrm{e}}\big((1 - c)G_0^{\mathrm{e}} + c\alpha_1^{\mathrm{e}}G_1^{\mathrm{e}}\big)\Delta\bar{\varepsilon},$$

where

$$(3.13) \qquad \alpha_1^{\mathrm{e}} = \frac{G_0^{\mathrm{e}} + G_*^{\mathrm{e}}}{G_1^{\mathrm{e}} + G_*^{\mathrm{e}}}, \qquad \alpha_0^{\mathrm{e}} = \frac{1}{1 - c + c\alpha_1^{\mathrm{e}}}, \qquad G_*^{\mathrm{e}} = \frac{G_0^{\mathrm{e}}(8G_0^{\mathrm{e}} + 9K_0^{\mathrm{e}})}{6(2G_0^{\mathrm{e}} + K_0^{\mathrm{e}})}.$$

The overall strain, denoted by $\bar{\varepsilon}_{\phi_0}$, for which the matrix reaches the limit of elastic regime, is evaluated by setting $\phi_0^{n+1} = 0$ and is equal to

$$(3.14) \qquad \bar{\varepsilon}_{\phi_0} = \bar{\varepsilon}|_{\phi_0=0} = \frac{\sigma_{\mathrm{y},0}}{2G_0^{\mathrm{e}}\alpha_0^{\mathrm{e}}}.$$

The corresponding overall stress $\bar{\sigma}_{\phi_0}^{\mathrm{e}}$ is then specified as

$$(3.15) \qquad \bar{\sigma}_{\phi_0}^{\mathrm{e}} = \bar{\sigma}|_{\phi_0=0} = \sigma_{\mathrm{y},0}\left(1 - c + c\alpha_1^{\mathrm{e}}\frac{G_1^{\mathrm{e}}}{G_0^{\mathrm{e}}}\right).$$

3.4. Elasto-plastic step

Let us consider now a step that involves the elastic-to-plastic transition. Accordingly, we have $\phi_0^n < 0$, $\phi_0^{n+1} = 0$, $\Delta\gamma_0 > 0$ and $G_0^{\mathrm{ep}} = G_0^{\mathrm{p}}$. Again, by solving Eqs. (3.5)–(3.9), the increments of strain and stress in the phases are obtained in the form

$$(3.16) \qquad \Delta\varepsilon_0 = \alpha_0^{\mathrm{p}}\Delta\bar{\varepsilon} - c\alpha_0^{\mathrm{p}}\beta_1^{\mathrm{p}}, \qquad \Delta\varepsilon_1 = \alpha_1^{\mathrm{p}}\Delta\varepsilon_0 + \beta_1^{\mathrm{p}},$$

$$(3.17) \qquad \Delta\sigma_0 = 2G_0^{\mathrm{p}}\Delta\varepsilon_0 + \Delta\sigma_0^{*}, \qquad \Delta\sigma_1 = 2G_1^{\mathrm{e}}\Delta\varepsilon_1,$$

where

$$(3.18) \qquad \alpha_1^{\mathrm{p}} = \frac{G_0^{\mathrm{p}} + G_*^{\mathrm{p}}}{G_1^{\mathrm{e}} + G_*^{\mathrm{p}}}, \qquad \alpha_0^{\mathrm{p}} = \frac{1}{1 - c + c\alpha_1^{\mathrm{p}}}, \qquad G_*^{\mathrm{p}} = \frac{G_0^{\mathrm{p}}(8G_0^{\mathrm{p}} + 9K_0^{\mathrm{e}})}{6(2G_0^{\mathrm{p}} + K_0^{\mathrm{e}})},$$

$$(3.19) \qquad G_0^{\mathrm{p}} = \frac{G_0^{\mathrm{e}}H_0}{2G_0^{\mathrm{e}} + H_0}, \qquad \Delta\sigma_0^{*} = 2G_0^{\mathrm{e}}\frac{\sigma_{\mathrm{y},0} - \sigma_0^n}{2G_0^{\mathrm{e}} + H_0}, \qquad \beta_1^{\mathrm{p}} = \frac{\Delta\sigma_0^{*}}{2(G_1^{\mathrm{e}} + G_*^{\mathrm{p}})}.$$

The increment $\Delta\gamma_0$ of plastic multiplier is determined from the yield condition $\phi_0^{n+1} = 0$. Using Eqs. (3.9) and (3.16)–(3.19), $\Delta\gamma_0$ is found equal to

$$(3.20) \qquad \Delta\gamma_0 = \frac{2G_0^{\mathrm{e}}}{2G_0^{\mathrm{e}} + H_0}\Delta\varepsilon_0 - \frac{\sigma_{\mathrm{y},0} - \sigma_0^n}{2G_0^{\mathrm{e}} + H_0}.$$

The overall strain $\bar{\varepsilon}_{\gamma_0}$ that would correspond to the elasto-plastic regime in the limit $\Delta\gamma_0 = 0$ can be determined from Eq. (3.20),

$$(3.21) \quad \bar{\varepsilon}_{\gamma_0} = \bar{\varepsilon}|_{\Delta\gamma_0=0} = \bar{\varepsilon}^n + (\sigma_{\mathrm{y},0} - \sigma_0^n)\left(\frac{1}{2G_0^{\mathrm{e}}\alpha_0^{\mathrm{p}}} + \frac{cG_0^{\mathrm{e}}}{(2G_0^{\mathrm{e}} + H_0)(G_1^{\mathrm{e}} + G_*^{\mathrm{p}})}\right),$$

where

$$(3.22) \qquad \bar{\varepsilon}^n = \frac{\sigma_0^n}{2G_0^{\mathrm{e}}\alpha_0^{\mathrm{e}}}.$$

3.5. Response discontinuity

Above we have determined two limit values of the overall strain, $\bar{\varepsilon}_{\phi_0}$ and $\bar{\varepsilon}_{\gamma_0}$, that are associated with the transition from the elastic to the plastic state in the matrix. Assuming that the matrix is in the elastic state, for $\bar{\varepsilon}^{n+1} < \bar{\varepsilon}_{\phi_0}$ we have $\phi_0^{n+1} < 0$ and $\Delta\gamma_0 = 0$. Assuming that the matrix is in the plastic state, for $\bar{\varepsilon}^{n+1} > \bar{\varepsilon}_{\gamma_0}$ we have $\phi_0^{n+1} = 0$ and $\Delta\gamma_0 > 0$. Clearly, each of the two states individually satisfies the complementarity conditions (3.10). A continuous transition from the elastic to the plastic state would be possible if the two limit strains were equal to each other so that for $\bar{\varepsilon}^{n+1} = \bar{\varepsilon}_{\phi_0} = \bar{\varepsilon}_{\gamma_0}$ we would have $\phi_0^{n+1} = 0$ and $\Delta\gamma_0 = 0$.

However, in general, the two limit strains are *not* equal to each other. Indeed, using Eqs. (3.14) and (3.21), the difference between the limit strains, referred to as the strain gap $\delta\bar{\varepsilon}$, is found equal to

$$(3.23) \quad \delta\bar{\varepsilon} = \bar{\varepsilon}_{\gamma_0} - \bar{\varepsilon}_{\phi_0} = c\alpha_0^e \left(\bar{\varepsilon}_{\phi_0} - \bar{\varepsilon}^n\right)\left(\alpha_1^p - \alpha_1^e + \frac{2(G_0^e)^2}{(2G_0^e + H_0)(G_1^e + G_*^p)}\right).$$

The strain gap $\delta\bar{\varepsilon}$ can be positive or negative depending on the sign of the last term in the parenthesis in Eq. (3.23). It can be verified that

$$(3.24) \qquad \delta\bar{\varepsilon} < 0 \quad \text{if } G_1^e > G_0^e \qquad \text{and} \qquad \delta\bar{\varepsilon} > 0 \quad \text{if } G_1^e < G_0^e.$$

The two situations are illustrated in Fig. 2. It has to be stressed that the sketch in Fig. 2 and the discussion that follows concern a single load step associated with the overall strain increment $\Delta\bar{\varepsilon}$ of varying length, and the initial state being characterized by $(\bar{\varepsilon}^n, \bar{\sigma}^n)$.

Case (a) in Fig. 2 corresponds to negative $\delta\bar{\varepsilon}$. It follows that two solutions of the governing equations exist for $\bar{\varepsilon}_{\gamma_0} \leq \bar{\varepsilon}^{n+1} \leq \bar{\varepsilon}_{\phi_0}$. Each solution corresponds to either elastic or plastic state in the matrix. The shaded zone indicates the range of strain increments in which two solutions are possible. In particular, it is shown in the bottom-left figure that in the shaded zone we have $\phi_0^{n+1} \leq 0$ and $\Delta\gamma_0 \geq 0$, thus both solutions satisfy the complementarity conditions (3.10) (the corresponding feasible branches are indicated by solid lines; the infeasible ones by dashed lines).

It is also indicated in Fig. 2 that each solution is associated with a distinct value of the overall stress. The related stress jump can be found in a closed form. However, the explicit formula is not provided here as it is rather lengthy. It can be verified that the stress jump $\delta\bar{\sigma}$ at $\bar{\varepsilon}^{n+1} = \bar{\varepsilon}_{\phi_0}$, defined as

$$(3.25) \qquad\qquad\qquad \delta\bar{\sigma} = \bar{\sigma}_{\phi_0}^p - \bar{\sigma}_{\phi_0}^e \qquad \text{if } \delta\bar{\varepsilon} < 0,$$

see Fig. 2, is always negative, $\delta\bar{\sigma} < 0$. Furthermore, the dependence of $\delta\bar{\sigma}$ on the previous strain $\bar{\varepsilon}^n$ is linear, and $\delta\bar{\sigma}$ is proportional to the term $(\bar{\varepsilon}_{\phi_0} - \bar{\varepsilon}^n)$, just like in the case of strain gap $\delta\bar{\varepsilon}$, see Eq. (3.23).
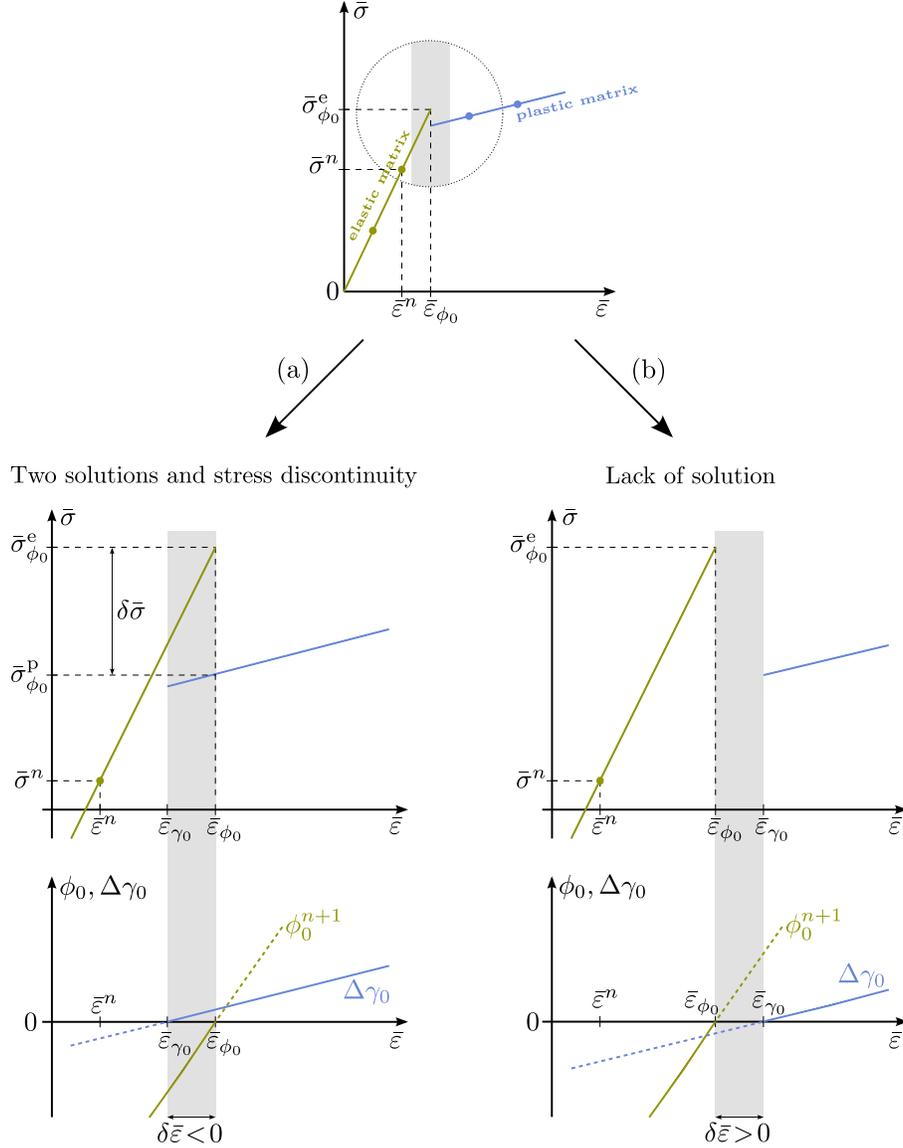
Fig. 2. Illustration of the response discontinuities at the elastic-to-plastic transition in the incremental Mori–Tanaka scheme. See text for explanations.

For a positive strain gap $\delta\bar{\varepsilon}$, see case (b) in Fig. 2, the governing equations have no solution for $\bar{\varepsilon}_{\phi_0} < \bar{\varepsilon}^{n+1} < \bar{\varepsilon}_{\gamma_0}$, and the corresponding range of strain increments is indicated by a shaded zone. In particular, in this zone, the complementarity conditions (3.10) are violated, i.e., either $\phi_0^{n+1} > 0$ or $\Delta\gamma_0 < 0$, as shown in the bottom-right figure.

3.6. Illustrative example

The analytical results derived above are illustrated by the following numerical example of a two-phase composite. The reference values of the material parameters used in the study are summarized in Table 1. The reference value of the volume fraction of spherical inclusions is $c = 0.1$.

Table 1. Reference values of material properties of the phases.

	Matrix ('0')	Inclusion ('1')
Bulk modulus, K_i^e [GPa]	65	240
Shear modulus, G_i^e [GPa]	30	180
Yield stress, $\sigma_{y,0}$ [MPa]	75	–
Hardening modulus, H_0 [MPa]	240	–

According to formula (3.23), the strain gap $\delta\bar{\varepsilon}$ is proportional to the term $(\bar{\varepsilon}_{\phi_0} - \bar{\varepsilon}^n)$. The stress jump $\delta\bar{\sigma}$ is also proportional to $(\bar{\varepsilon}_{\phi_0} - \bar{\varepsilon}^n)$. Accordingly, the numerical results are presented below for $\bar{\varepsilon}^n = 0$ (which corresponds to $\bar{\sigma}^n = 0$), i.e., as if the elastic-to-plastic transition was approached in one step. The values of $\delta\bar{\varepsilon}$ and $\delta\bar{\sigma}$ corresponding to $0 < \bar{\varepsilon}^n < \bar{\varepsilon}_{\phi_0}$ can be simply obtained by scaling those results by the factor $(\bar{\varepsilon}_{\phi_0} - \bar{\varepsilon}^n)/\bar{\varepsilon}_{\phi_0}$.

The dependence of the normalized strain gap $\delta\bar{\varepsilon}/\bar{\varepsilon}_{\phi_0}$ on the elastic shear moduli ratio G_1^e/G_0^e is shown in Fig. 3a for $G_1^e/G_0^e \leq 1$ and in Fig. 3b for $G_1^e/G_0^e \geq 1$. Here, the material parameters for the matrix are those presented in Table 1, and the elastic shear modulus G_1^e of inclusions is varied in a wide range. Let us note that the strain gap $\delta\bar{\varepsilon}$ does not depend on the bulk modulus of inclusions, cf. Eq. (3.23). Additionally, the influence of the hardening modulus of the matrix H_0, normalized by the elastic shear modulus G_0^e, is also presented in Fig. 3, the ratio of $H_0/G_0^e = 0.008$ corresponding to the reference parameters given in Table 1.

When $G_1^e/G_0^e = 1$, there is no strain gap, $\delta\bar{\varepsilon} = 0$. For higher values of this ratio, the strain gap $\delta\bar{\varepsilon}$ is negative, and the two solutions are possible according to the scheme shown in Fig. 2a. On the contrary, if $G_1^e/G_0^e < 1$, the strain gap $\delta\bar{\varepsilon}$ is positive, and no solution exists for $\bar{\varepsilon}_{\phi_0} < \bar{\varepsilon}^{n+1} < \bar{\varepsilon}_{\gamma_0}$, see Fig. 2b.

As it is shown in Fig. 3a, for the limit case of a porous material, i.e. for $G_1^e = 0$, strain gap has a finite value. This value depends on the hardening modulus of the matrix, and it increases significantly as the hardening modulus H_0 decreases to zero. For instance, $\delta\bar{\varepsilon}/\bar{\varepsilon}_{\phi_0} \approx 15.3$ for $G_1^e = 0$ and for the reference ratio of $H_0/G_0^e = 0.008$. Accordingly, the solution does not exist for a large range of strain increments.

The case when two solutions may exist is presented in Fig. 3b. Here, the magnitude of the (now negative) strain gap is approximately three orders of

magnitude smaller compared to the case of no solution, cf. Fig. 3a. Additionally, the strain gap is by far less sensitive to the hardening modulus of the matrix, see Fig. 3b. The strain gap vanishes for rigid inclusions, i.e., for $G_1^e/G_0^e \to \infty$.
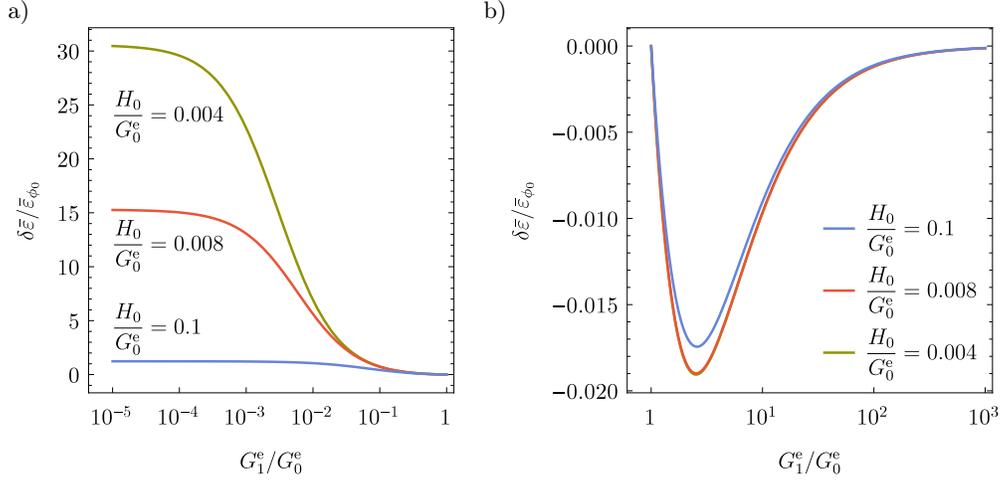
Fig. 3. Normalized strain gap $\delta\bar{\varepsilon}/\bar{\varepsilon}_{\phi_0}$ as a function of the ratio of elastic shear moduli: a) $G_1^e/G_0^e \leq 1$ and b) $G_1^e/G_0^e \geq 1$.

The effect of Poisson's ratio ν_0 on the strain gap is shown in Fig. 4. Here, the shear modulus G_0^e is fixed at the reference value given in Table 1, and the bulk modulus K_0^e is varied according to the varying value of ν_0. The dependence
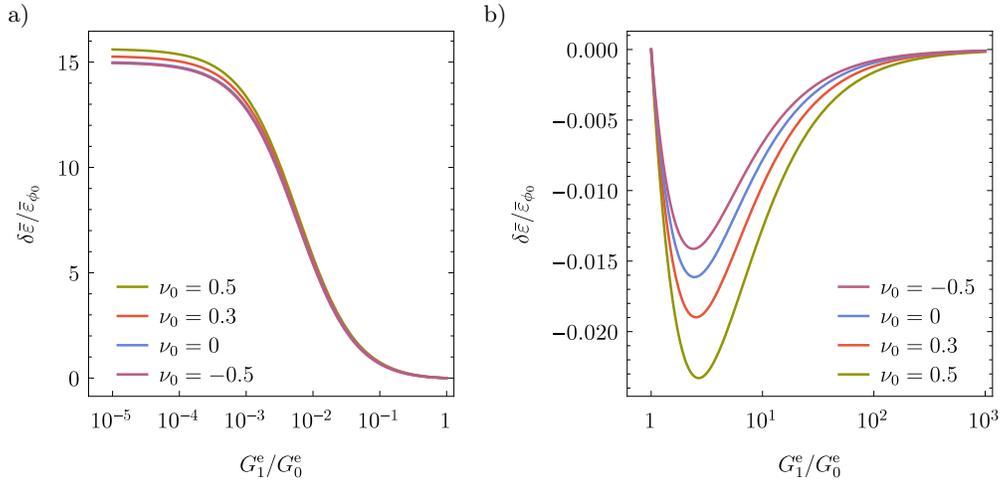
Fig. 4. Effect of Poisson's ratio ν_0 on the normalized strain gap $\delta\bar{\varepsilon}/\bar{\varepsilon}_{\phi_0}$ for a) $G_1^e/G_0^e \leq 1$ and b) $G_1^e/G_0^e \geq 1$.

of $\delta\bar{\varepsilon}/\bar{\varepsilon}_{\phi_0}$ on $G_1^{\mathrm{e}}/G_0^{\mathrm{e}}$ is similar to that shown in Fig. 3. The effect of ν_0 is more pronounced for $G_1^{\mathrm{e}}/G_0^{\mathrm{e}} > 1$ than for $G_1^{\mathrm{e}}/G_0^{\mathrm{e}} < 1$.

The dependence of the normalized stress jump $\delta\bar{\sigma}/\sigma_{\mathrm{y},0}$ on the ratio $G_1^{\mathrm{e}}/G_0^{\mathrm{e}}$ is shown in Fig. 5. Note that $\delta\bar{\sigma}$ is defined only for $\delta\bar{\varepsilon} \leq 0$, i.e. for $G_1^{\mathrm{e}}/G_0^{\mathrm{e}} \geq 1$. The effect of the hardening modulus H_0 and Poisson's ratio ν_0 is also depicted. It can be seen that for rigid inclusions ($G_1^{\mathrm{e}}/G_0^{\mathrm{e}} \to \infty$) the stress jump $\delta\bar{\sigma}$ is of the order of $0.1\sigma_{\mathrm{y},0}$, which is a considerably large value. Let us note that the stress jump $\delta\bar{\sigma}$ is finite for $G_1^{\mathrm{e}}/G_0^{\mathrm{e}} \to \infty$, even though the strain gap $\delta\bar{\varepsilon}$ is tending to 0 in this case, cf. Figs. 3b and 4b.

a)

b)
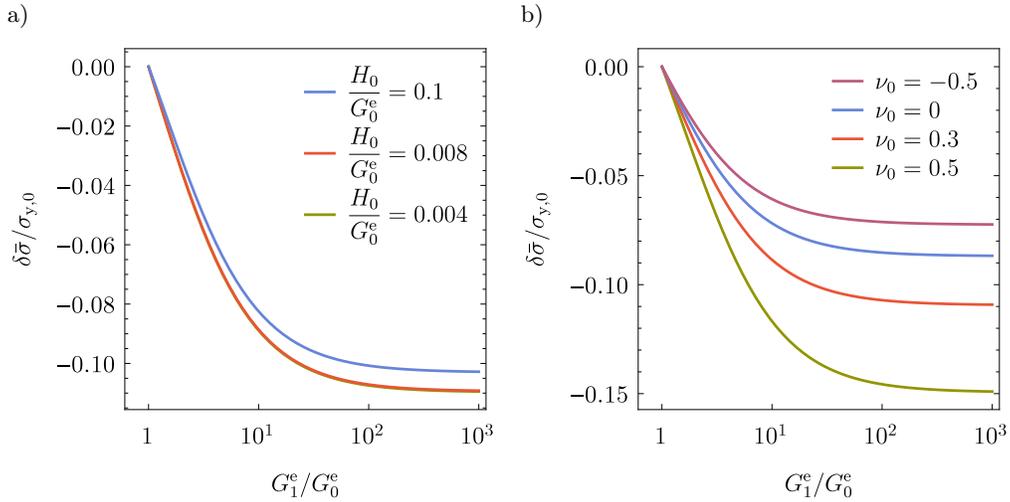
FIG. 5. Normalized stress jump $\delta\bar{\sigma}/\sigma_{\mathrm{y},0}$ as a function of the elastic shear moduli ratio $G_1^{\mathrm{e}}/G_0^{\mathrm{e}} \geq 1$. The effect of the normalized hardening coefficient H_0/G_0^{e} (a) and Poisson's ratio ν_0 (b) is also shown.

3.7. Alternative formulations of the incremental MT scheme

The detailed analysis presented above concerns the specific formulation of the incremental MT scheme adopted in Section 3.2. As already mentioned, the finite-step scheme can be formulated in several versions, and in this section we briefly discuss the influence of the formulation itself on the response discontinuities.

The coefficient P^{ep}, Eq. $(3.6)_2$, derived from the polarization tensor $\mathbb{P}$ corresponds to the isotropization of the elasto-plastic tangent $\mathbb{L}_0^{\mathrm{ep}}$ according to Eq. (B.1). If the alternative isotropization method, see Eq. (B.2), is adopted, then P^{ep} takes the following form:

$$(3.26) \qquad P^{\mathrm{ep}} = \frac{3(2\overline{G}_0 + K_0^{\mathrm{e}})}{5\overline{G}_0(4\overline{G}_0 + 3K_0^{\mathrm{e}})}, \qquad \overline{G}_0 = \frac{1}{5}(4G_0^{\mathrm{e}} + G_0^{\mathrm{ep}}).$$

It can be verified that in this case we have

$$(3.27) \qquad \delta\bar{\varepsilon} < 0 \quad \text{if } G_1^e < G_0^e \qquad \text{and} \qquad \delta\bar{\varepsilon} > 0 \quad \text{if } G_1^e > G_0^e,$$

so that the sign of the strain gap $\delta\bar{\varepsilon}$ is opposite to that in the case of isotropization (B.1), see Eq. (3.24). The sign of the stress jump $\delta\bar{\sigma}$, which is now defined for $G_1^e < G_0^e$, see Eq. (3.25), depends on material parameters through the following expression:

$$(3.28) \qquad \text{sign}(\delta\bar{\sigma}) = -\text{sign}\big((G_1^e - G_0^e)((G_1^e - G_0^e)H_0 + 2G_1^e G_0^e)\big),$$

and can be either positive or negative.

Another version of the incremental MT scheme is obtained when the interaction equation (2.9) is replaced by its transformed form (2.11), cf. [23, 38]. In that case, the strain gap can be expressed in the following form:

$$(3.29) \qquad \delta\bar{\varepsilon} = c\alpha_0^e\,(\bar{\varepsilon}_{\phi_0} - \bar{\varepsilon}^n)(\alpha_1^p - \alpha_1^e),$$

and $\delta\bar{\varepsilon}$ is negative independently of the isotropization method, $(3.6)_2$ or (3.26). Accordingly, there are always two solutions and a non-zero stress jump $\delta\bar{\sigma}$ of the sign specified by

$$(3.30) \qquad \text{sign}(\delta\bar{\sigma}) = -\text{sign}((G_1^e - G_0^e)H_0 + 2G_1^e G_0^e).$$

Concluding, the finite-step incremental MT scheme exhibits the response discontinuities regardless of the details of the formulation. Those details influence the specific qualitative and quantitative features, for instance, the sign of the strain gap $\delta\bar{\varepsilon}$.

4. Possible remedies

The response discontinuities discussed above constitute a highly undesirable feature of the incremental MT scheme. This particularly concerns application of the incremental MT scheme as a material model in finite element computations. Some remedies are discussed below.

As shown in Section 3.5, the strain gap $\delta\bar{\varepsilon}$ and the associated stress jump $\delta\bar{\sigma}$ depend on the stress state at the end of the previous step. In particular, $\delta\bar{\varepsilon}$ and $\delta\bar{\sigma}$ are proportional to the term $(\bar{\varepsilon}_{\phi_0} - \bar{\varepsilon}^n)$, so that both gaps decrease when $\bar{\varepsilon}^n$ gets closer to $\bar{\varepsilon}_{\phi_0}$. The problems related to response discontinuities may thus be reduced by reducing the load increments. However, apart from increasing the computational cost, this does not solve the problem completely as the problems may still be encountered, though with a lower probability.

Let us note that in a typical medium- or large-scale finite element computation there are thousands or even millions of integration (Gauss) points at which the constitutive model is evaluated at each time increment and at each global Newton iteration. Accordingly, even if the problematic range of strain increments is small, the probability of encountering the discontinuity is in practice high.

The response discontinuities are caused by the jump of the tangent stiffness of the matrix in the elastic-to-plastic transition. The jump can be reduced by adopting the generalized mid-point rule (2.8) and by formulating the interaction equation (2.9) in terms of the tangent operator $\mathbb{L}_0^{\mathrm{ep},n+\theta}$ with $\theta < 1$. For instance, the mid-point rule ($\theta = 0.5$) has been used in [23], and a heuristic approach for determining θ has been proposed in [37].

Let us consider again the proportional deviatoric loading discussed in Section 3. In case of the elasto-plastic step, the tangent modulus G_0^{ep} corresponding to the generalized mid-point rule takes the form

$$(4.1) \qquad G_0^{\mathrm{ep}} = (1 - \theta)G_0^{\mathrm{e}} + \theta G_0^{\mathrm{p}},$$

and the scalar coefficients G_*^{ep} and P^{ep} defined by Eq. (3.6) are then expressed in terms of G_0^{ep} defined above. With the above redefinition, the remaining formulae corresponding to the elasto-plastic step, cf. Section 3.4, are not changed. The form of Eqs. (3.23)–(3.25) that characterize the response discontinuities also remains unchanged.

Application of the generalized mid-point rule indeed reduces the range of strains in which response discontinuities occur. This is illustrated in Fig. 6 for the case of $\theta = 0.5$. The normalized strain gap $\delta\bar{\varepsilon}/\bar{\varepsilon}_{\phi_0}$ is significantly smaller
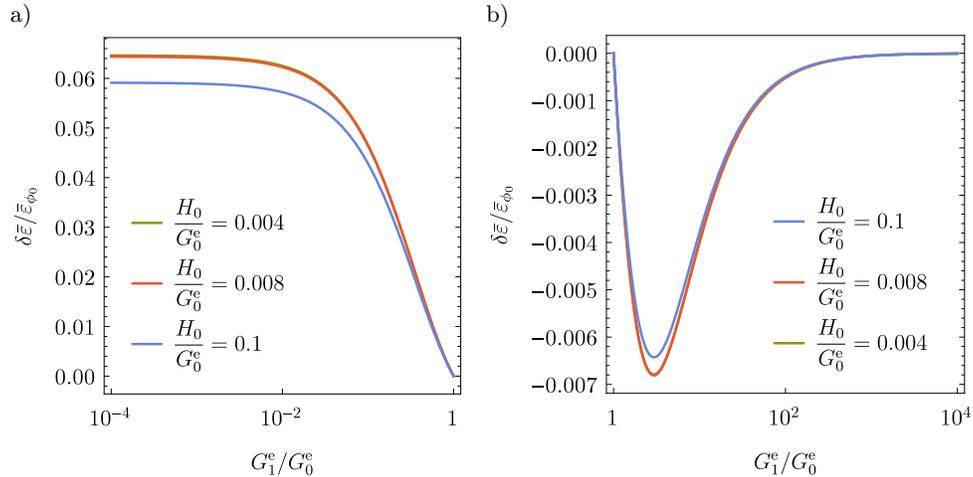
Fig. 6. Normalized strain gap $\delta\bar{\varepsilon}/\bar{\varepsilon}_{\phi_0}$ corresponding to the mid-point rule (4.1) for $\theta = 0.5$: a) $G_1^{\mathrm{e}}/G_0^{\mathrm{e}} \leq 1$ and b) $G_1^{\mathrm{e}}/G_0^{\mathrm{e}} \geq 1$.

a)

b)
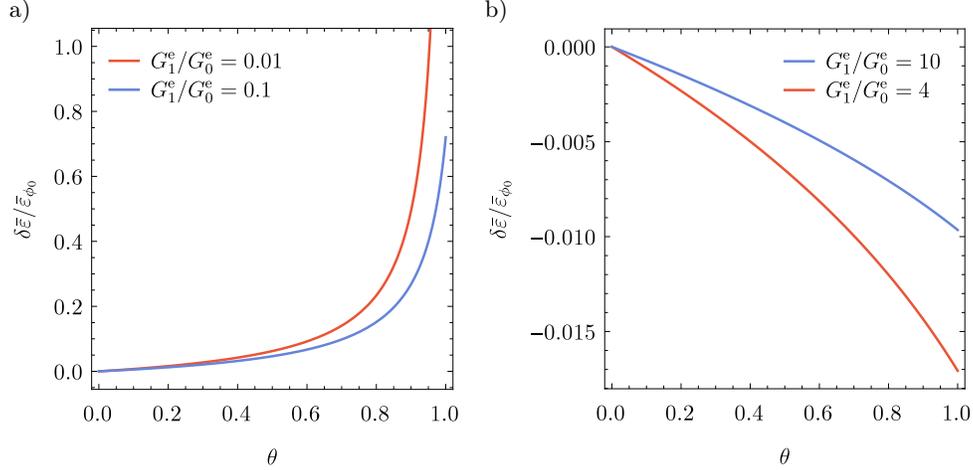
Fig. 7. Normalized strain gap $\delta\bar\varepsilon/\bar\varepsilon_{\phi_0}$ as a function of parameter θ for the fixed ratio of elastic shear moduli and for $H_0/G_0^{\mathrm{e}} = 0.008$.

than in the case of $\theta = 1$ shown in Fig. 3, but it is not equal to zero. Dependence of the strain gap $\delta\bar\varepsilon/\bar\varepsilon_{\phi_0}$ on θ is illustrated in Fig. 7 for selected values of the ratio $G_1^{\mathrm{e}}/G_0^{\mathrm{e}}$.

It follows that the problems related to response discontinuities cannot be completely avoided by applying the mid-point rule, and convergence problems can be easily encountered in middle- or large-scale computations. Referring to the illustrative example reported in Fig. 1, for the mid-point rule with $\theta = 0.5$ (the corresponding results are not provided for brevity), the number of steps needed to complete the simulation was equal to 15. The MT scheme employing the mid-point rule is thus more robust than the basic MT scheme that corresponds to $\theta = 1$ (49 steps, Fig. 1a). At the same time, it is not as robust as the MT scheme employing the substepping strategy that is described below (10 steps, Fig. 1b).

An ultimate remedy to the problem of response discontinuities, applicable in a general case of multiaxial, non-monotonic and non-radial loading, is to split the step involving the elastic-to-plastic transition into two substeps. Specifically, in a strain-controlled process with a prescribed strain increment $\Delta\bar\varepsilon$, such that $\bar\varepsilon^{n+1} = \bar\varepsilon^n + \Delta\bar\varepsilon$, the following two substeps are considered,

$$(4.2) \qquad \bar\varepsilon^{n+\beta} = \bar\varepsilon^n + \beta\Delta\bar\varepsilon, \qquad \bar\varepsilon^{n+1} = \bar\varepsilon^{n+\beta} + (1-\beta)\Delta\bar\varepsilon, \qquad \beta \in (0,1).$$

The first substep is purely elastic and ends exactly at the instant of the elastic-to-plastic transition. The fraction β is determined from the condition $\phi_0^{n+\beta} = 0$. The second substep proceeds then purely in the plastic regime. Substepping is not needed in case of a purely elastic or purely plastic step.

When the inclusions are elastic, implementation of the substepping scheme is relatively straightforward. In brief, a trial elastic step is first considered, for which the equations of the MT model are solved in a closed form. If the yield condition $\phi_0^{n+1} \leq 0$ is violated, then the step is elastic-plastic, and parameter β is determined from the condition $\phi_0^{n+\beta} = 0$. Importantly, the substepping procedure admits exact linearization.

The incremental MT scheme enhanced by the above substepping strategy has been successfully implemented in a finite element code, and its efficiency and robustness in three-dimensional finite element computations have been demonstrated in [39]. An illustrative example taken from [39] has been provided in Section 3.1, cf. Fig. 1.

In the case of proportional deviatoric loading discussed in Section 3 and for linear hardening, the substepping scheme discussed above yields an exact response for arbitrarily large strain increments.

5. Conclusion

The incremental Mori–Tanaka model of elasto-plastic composites has been discussed with the focus on its finite-step formulation. The sudden change of the elasto-plastic tangent moduli at the instant of the elastic-to-plastic transition in the matrix has been shown to lead to discontinuities in the overall response. Specifically, depending on the details of the formulation and on the properties of the phases, the incremental finite-step equations may have two solutions or no solution. In the former case, switching between the two solutions is associated with a jump in the overall stress. The discontinuities are encountered in a specific range of overall strain increments in the vicinity of the elastic-to-plastic transition.

The related effects have been studied in detail for a special case of proportional deviatoric loading in which the constitutive equations and the equations of the micro–macro transition scheme can be formulated in a scalar form. As a result, the incremental equations can be solved in a closed form, and compact expressions for the quantities characterizing the response discontinuities have been derived.

The discontinuities constitute an undesirable feature of the incremental Mori–Tanaka scheme that has not been discussed in the literature so far. In particular, the discontinuities impose a severe constraint on the maximum strain increment that can effectively be employed in large-scale finite element computations employing the incremental Mori–Tanaka scheme. Some remedies to the related problems have been briefly discussed. In particular, a substepping strategy leads to an efficient and robust finite element implementation, as demonstrated by Sadowski *et al.* [39].

A. Elasto-plastic tangent moduli and polarization tensor

In the analysis of Section 3, the matrix phase '0' is assumed to obey the J_2 plasticity model with linear isotropic hardening. The corresponding constitutive relations are summarized as follows:

$$(A.1) \quad \dot{\boldsymbol{\sigma}}_0 = \mathbb{L}_0^{\mathrm{e}}(\dot{\boldsymbol{\varepsilon}}_0 - \dot{\boldsymbol{\varepsilon}}_0^{\mathrm{p}}), \quad \dot{\boldsymbol{\varepsilon}}_0^{\mathrm{p}} = \dot{\gamma}_0 \frac{\partial \phi_0}{\partial \boldsymbol{\sigma}_0}, \quad \phi_0 \leq 0, \quad \dot{\gamma}_0 \geq 0, \quad \dot{\gamma}_0 \phi_0 = 0,$$

where

$$(A.2) \qquad \phi_0 = \|\boldsymbol{\sigma}_0'\| - (\sigma_{y,0} + H_0 \gamma_0), \qquad \mathbf{N}_0 = \frac{\partial \phi_0}{\partial \boldsymbol{\sigma}_0} = \frac{\boldsymbol{\sigma}_0'}{\|\boldsymbol{\sigma}_0'\|},$$

and $\boldsymbol{\sigma}_0'$ is the stress deviator. Note that, in the definition above, the yield stress $\sigma_{y,0}$ is related to the uniaxial yield stress Y by $\sigma_{y,0} = \sqrt{\frac{2}{3}} Y$, and the hardening modulus H_0 is defined accordingly.

The plastic multiplier $\dot{\gamma}_0$ is determined from the consistency condition $\dot{\phi}_0 = 0$, and the rate form (2.4) of the constitutive relation is obtained, in which the elasto-plastic tangent stiffness tensor has the following form:

$$(A.3) \quad \mathbb{L}_0^{\mathrm{ep}} = \begin{cases} 3K_0^{\mathrm{e}} \, \mathbb{I}^{\mathrm{P}} + 2G_0^{\mathrm{e}} \, \mathbb{I}^{\mathrm{D}} & \text{for } \dot{\gamma}_0 = 0, \\ 3K_0^{\mathrm{e}} \, \mathbb{I}^{\mathrm{P}} + 2G_0^{\mathrm{e}}(\mathbb{I}^{\mathrm{D}} - \mathbf{N}_0 \otimes \mathbf{N}_0) + 2G_0^{\mathrm{p}} \, \mathbf{N}_0 \otimes \mathbf{N}_0 & \text{for } \dot{\gamma}_0 > 0, \end{cases}$$

where

$$(A.4) \qquad G_0^{\mathrm{p}} = \frac{G_0^{\mathrm{e}} H_0}{2G_0^{\mathrm{e}} + H_0}, \qquad \mathbb{I}^{\mathrm{P}} = \frac{1}{3} \mathbf{1} \otimes \mathbf{1}, \qquad \mathbb{I}^{\mathrm{D}} = \mathbb{I} - \frac{1}{3} \mathbf{1} \otimes \mathbf{1},$$

and $\mathbb{I}$ is the symmetrized fourth-order identity tensor.

As it is seen, $\mathbb{L}_0^{\mathrm{ep}}$ tensor is in general anisotropic (orthotropic), so that the corresponding polarisation tensor $\mathbb{P}$ would have to be calculated employing numerical integration. Anyway, isotropization of the elasto-plastic tangent is usually performed in order to avoid excessively stiff response, see Appendix B. The isotropized tangent stiffness has the form:

$$(A.5) \qquad \mathbb{L}_0^{\mathrm{ep(iso)}} = 3K_0^{\mathrm{e}} \, \mathbb{I}^{\mathrm{P}} + 2G_0^{\mathrm{ep(iso)}} \, \mathbb{I}^{\mathrm{D}},$$

where specification of the modulus $G_0^{\mathrm{ep(iso)}}$ depends on the adopted isotropization method, see Eqs. (B.1) and (B.2) in Appendix B. In the case of spherical inclusions and isotropic stiffness tensor, the polarization tensor $\mathbb{P}$ is also isotropic and is given in the following closed form:

$$(A.6) \qquad \mathbb{P}^{\mathrm{(iso)}} = \hat{\mathbb{P}}(\mathbb{L}_0^{\mathrm{ep(iso)}}) = P_{\mathrm{vol}}^{\mathrm{e}} \mathbb{I}^{\mathrm{P}} + P^{\mathrm{ep}} \, \mathbb{I}^{\mathrm{D}},$$

where

$$(A.7) \qquad P^{\text{e}}_{\text{vol}} = \frac{1}{3K^{\text{e}}_0 + 4G^{\text{ep(iso)}}_0}, \qquad P^{\text{ep}} = \frac{3}{5G^{\text{ep(iso)}}_0} \frac{K^{\text{e}}_0 + 2G^{\text{ep(iso)}}_0}{3K^{\text{e}}_0 + 4G^{\text{ep(iso)}}_0}.$$

The Hill tensor $\mathbb{L}^{\text{ep}}_*$ in the interaction equation (2.5) is then calculated from Eq. (2.6) with $\mathbb{P} = \mathbb{P}^{(\text{iso})}$,

$$(A.8) \qquad \mathbb{L}^{\text{ep}}_* = \mathbb{P}^{(\text{iso})^{-1}} - \mathbb{L}^{\text{ep}}_0,$$

and an analogous treatment is applied in the case of the finite-step formulation of Section 2.3.

Let us consider now the proportional deviatoric loading specified by the direction $\mathbf{N}$, see Eq. (3.1). Since the tensors $\mathbb{L}^{\text{ep}}_0$ and $\mathbb{L}^{\text{ep}}_*$ are coaxial it can be shown that the stress and strain rates in the phases also have the direction $\mathbf{N}$, see Eq. (3.4), and, in particular, in the plastic state we have

$$(A.9) \qquad \mathbf{N}_0 = \mathbf{N}.$$

As a result, the process can be described by the set of scalar equations, as discussed in Section 3. The elasto-plastic response of the matrix is then characterized by the elasto-plastic tangent shear modulus G^{ep}_0 defined by

$$(A.10) \qquad G^{\text{ep}}_0 = \frac{1}{2}\mathbf{N} \cdot \mathbb{L}^{\text{ep}}_0 \mathbf{N} = \begin{cases} G^{\text{e}}_0 & \text{for } \dot{\gamma}_0 = 0, \\ G^{\text{p}}_0 & \text{for } \dot{\gamma}_0 > 0, \end{cases}$$

while the coefficient in the scalar interaction equation (3.5) is given by

$$(A.11) \qquad G^{\text{ep}}_* = \frac{1}{2}\mathbf{N} \cdot \mathbb{L}^{\text{ep}}_* \mathbf{N} = \frac{1}{2P^{\text{ep}}} - G^{\text{ep}}_0.$$

B. Isotropization

As mentioned in Section 2.2, the elasto-plastic tangent moduli tensor $\mathbb{L}^{\text{ep}}_0$ is usually isotropized, and the polarization tensor $\mathbb{P}$ is evaluated in terms of the corresponding isotropic tensor $\mathbb{L}^{\text{ep(iso)}}_0$. As a result, an excessively stiff response is avoided [23, 24, 42].

Two methods of isotropization are here briefly recalled. In both methods, the bulk modulus of the isotropized tangent is equal to the elastic bulk modulus of the matrix. As far as the isotropized shear modulus is concerned, in the first method it is calculated as a projection of the tangent elasto-plastic stiffness onto the unit normal $\mathbf{N}_0$ to the yield surface ϕ_0 [24, 43],

$$(B.1) \qquad G^{\text{ep(iso)}}_0 = \frac{1}{2}\mathbf{N}_0 \cdot \mathbb{L}^{\text{ep}}_0 \mathbf{N}_0, \qquad \mathbf{N}_0 = \frac{\mathbf{n}_0}{\|\mathbf{n}_0\|}, \qquad \mathbf{n}_0 = \frac{\partial \phi_0}{\partial \boldsymbol{\sigma}_0}.$$

Consequently, the coefficient P^{ep} derived from the polarization tensor $\mathbb{P}$ is given by the formula $(3.6)_2$. In the second method [23, 44], the isotropized shear modulus is determined according to

$$(\text{B.2}) \qquad G_0^{\mathrm{ep(iso)}} = \frac{1}{10}\left(L_{0,ijij}^{\mathrm{ep}} - \frac{1}{3}L_{0,iijj}^{\mathrm{ep}} \right)$$

and the coefficient P^{ep} is then defined by Eq. (3.26). The first method leads to softer predictions and is more often used in the literature [23, 24, 45] because it gives more reliable predictions.

Acknowledgment

References

1. T. Mori, K. Tanaka, *Average stress in matrix and average elastic energy of materials with misfitting inclusions*, Acta Metallurgica, **21**, 571–574, 1973.

2. Y. Benveniste, *A new approach to the application of Mori-Tanaka's theory in composite materials*, Mechanics of Materials, **6**, 147–157, 1987.

3. E. Kröner, *Berechnung der elastischen konstanten des vielkristalls aus den konstanten des einkristalls*, Zeitschrift für Physik, **151**, 504–518, 1958.

4. R. Hill, *A self-consistent mechanics of composite materials*, Journal of the Mechanics and Physics of Solids, **13**, 213–222, 1965.

5. R.M. Christensen, K.H. Lo, *Solutions for effective shear properties in three phase sphere and cylinder models*, Journal of the Mechanics and Physics of Solids, **27**, 315–330, 1979.

6. E. Herve, A. Zaoui, *Modelling the effective behavior of non-linear matrix-inclusion composites*, European Journal of Mechanics A/Solids, **9**, 505–516, 1990.

7. R. McLaughlin, *A study of the differential scheme for composite materials*, International Journal of Engineering Science, **15**, 237–244, 1977.

8. A. Broohm, P. Zattarin, P. Lipinski, *Prediction of mechanical behaviour of inhomogeneous and anisotropic materials using an incremental scheme*, Archives of Mechanics, **6**, 949–967, 2000.

9. M. Cherkaoui, H. Sabar, M. Berveiller, *Micromechanical approach of the coated inclusion problem and applications to composite materials*, Journal of Engineering Materials and Technology, **116**, 274–278, 1994.

10. M. Hori, S. Nemat-Nasser, *Double-inclusion model and overall moduli of multi-phase composites*, Mechanics of Materials, **14**, 189–206, 1993.

11. F. Feyel, J.L. Chaboche, *FE^2 multiscale approach for modelling the elastoviscoplastic behaviour of long fibre SiC/Ti composite materials*, Computer Methods in Applied Mechanics and Engineering, **183**, 309–330, 2000.

12. V. Kouznetsova, W.A.M. Brekelmans, F.P.T. Baaijens, *An approach to micro-macro modeling of heterogeneous materials*, Computational Mechanics, **27**, 37–48, 2001.

13. G.J. Dvorak, Y. Benveniste, *On transformation strains and uniform fields in multi-phase elastic media*, Proceedings of the Royal Society of London A, **437**, 291–310, 1992.

14. J.W. Hutchinson, *Bounds and self-consistent estimates for creep of polycrystalline materials*, Proceedings of the Royal Society of London A, **348**, 101–127, 1976.

15. G.P. Tandon, G.J. Weng, *A theory of particle-reinforced plasticity*, Transactions of the ASME Journal of Applied Mechanics, **55**, 126–135, 1988.

16. A. Molinari, G.R. Canova, S.Ahzi, *A self consistent approach of the large deformation polycrystal viscoplasticity*, Acta Metallurgica, **35**, 2983–2994, 1987.

17. R.A. Lebensohn, C.N. Tomé, *A self-consistent anisotropic approach for the simulation of plastic deformation and texture development of polycrystals: Application to zirconium alloys*, Acta Metallurgica et Materialia, **41**, 2611–2624, 1993.

18. R. Masson, A. Zaoui, *Self-consistent estimates of the rate-dependent elasto-plastic behaviour of polycrystalline materials*, Journal of the Mechanics and Physics of Solids, **47**, 1543–1568, 1999.

19. R. Masson, M. Bornert, P. Suquet, A. Zaoui, *An affine formulation for the prediction of the effective properties of nonlinear composites and polycrystals*, Journal of the Mechanics and Physics of Solids, **48**, 1203–1227, 2000.

20. J.L. Chaboche, S. Kruch, J.F. Maire, T. Pottier, *Towards a micromechanics based inelastic and damage modeling of composites*, International Journal of Plasticity, **17**, 411–439, 2001.

21. A. Molinari, *Averaging models for heterogeneous viscoplastic and elastic viscoplastic materials*, Transactions of the ASME Journal of Engineering Materials and Technology, **124**, 62–70, 2002.

22. K. Kowalczyk-Gajewska, H. Petryk, *Sequential linearization method for viscous/elastic heterogeneous materials*, European Journal of Mechanics A/Solids, **30**, 650–664, 2011.

23. I. Doghri, A. Ouaar, *Homogenization of two-phase elasto-plastic composite materials and structures: Study of tangent operators, cyclic plasticity and numerical algorithms*, International Journal of Solids and Structures, **40**, 1681–1712, 2003.

24. J.L. Chaboche, P. Kanouté, A. Roos, *On the capabilities of mean-field approaches for the description of plasticity in metal matrix composites*, International Journal of Plasticity, **21**, 1409–1434, 2005.

25. I. Doghri, L. Adam, N. Bilger, *Mean-field homogenization of elasto-viscoplastic composites based on a general incrementally affine linearization method*, International Journal of Plasticity, **26**, 219–238, 2010.

26. C. Czarnota, K. Kowalczyk-Gajewska, A. Salahouelhadj, M. Martiny, S. Mercier, *Modeling of the cyclic behavior of elastic–viscoplastic composites by the additive tangent Mori–Tanaka approach and validation by finite element calculations*, International Journal of Solids and Structures, **56–57**, 96–117, 2015.

27. G. Ravichandran, C.T. Liu, *Modelling constitutive behavior of particulate composites undergoing damage*, International Journal of Solids and Structures, **32**, 979–990, 1995.

28. C. Garion, B. Skoczeń, S. Sgobba, *Constitutive modelling and identification of parameters of the plastic strain-induced martensitic transformation in 316L stainless steel at cryogenic temperatures*, International Journal of Plasticity, **22**, 1234–1264, 2006.

29. L. Delannay, P. Jacques, T. Pardoen, *Modelling of the plastic flow of trip-aided multiphase steel based on an incremental mean-field approach*, International Journal of Solids and Structures, **45**, 1825–1843, 2008.

30. J.G. Boyd, D.C. Lagoudas, *A thermodynamical constitutive model for shape memory materials. Part II. The SMA composite material*, International Journal of Plasticity, **12**, 843–873, 1996.

31. A.H.Y. Lue, Y. Tomota, M. Taya, K. Inoue, T. Mori, *Micro-mechanic modeling of the stress–strain curves of a TiNiCu shape memory alloy*, Materials Science and Engineering A, **285**, 326–337, 2000.

32. G.K. Hu, Q.P. Sun, *Thermal expansion of composites with shape memory alloy inclusions and elastic matrix*, Composites: Part A, **33**, 717–724, 2002.

33. H.E. Pettermann, C.O. Huber, M.H. Luxner, S. Nogales, H.J. Böhm, *An incremental Mori–Tanaka homogenization scheme for finite strain thermoelastoplasticity of MMCs*, Materials, **3**, 434–451, 2010.

34. I. Doghri, M.I. El Ghezal, L. Adam, *Finite strain mean-field homogenization of composite materials with hyperelastic-plastic constituents*, International Journal of Plasticity, **81**, 40–62, 2016.

35. H.E. Pettermann, A.F. Plankensteiner, H.J. Böhm, F.G. Rammerstorfer, *A thermo-elasto-plastic constitutive law for inhomogeneous materials based on an incremental Mori–Tanaka approach*, Computers and Structures, **71**, 197–214, 1999.

36. J.D. Eshelby, *The determination of the elastic field of an ellipsoidal inclusion, and related problems*, Proceedings of the Royal Society of London A, **241**, 376–396, 1957.

37. L. Delannay, I. Doghri, O. Pierard, *Prediction of tension–compression cycles in multiphase steel using a modified incremental mean-field model*, International Journal of Solids and Structures, **44**, 7291–7306, 2007.

38. L. Brassart, *Homogenization of elasto-(visco)plastic composites: history-dependent incremental and variational approaches*, Ph.D. thesis, Université catholique de Louvaino, Louvain-la-Neuve, Belgium, 2011.

39. P. Sadowski, K. Kowalczyk-Gajewska, S. Stupkiewicz, *Consistent treatment and automation of the incremental Mori–Tanaka scheme for elasto-plastic composites*, submitted 2017.

40. J.R. Willis, *Variational and Related Methods for the Overall Properties of Composites*, Vol. 21 of Advances in Applied Mechanics, Academic Press, New York, 1981.

41. O. Pierard, C. González, J. Segurado, J. LLorca, I. Doghri, *Micromechanics of elasto-plastic materials reinforced with ellipsoidal inclusions*, International Journal of Solids and Structures, **44**, 6945–6962, 2007.

42. O. Pierard, I. Doghri, *Study of various estimates of the macroscopic tangent operator in the incremental homogenization of elastoplastic composites*, International Journal for Multiscale Computational Engineering, **4**, 521–543, 2006.

43. C. González, J. LLorca, *A self-consistent approach to the elasto-plastic behaviour of two-phase materials including damage*, Journal of the Mechanics and Physics of Solids, **48**, 675–692, 2000.

44. M. Bornert, *Homogeneisation des milieux aleatoires; bones et estimations*, [in:] M. Bornert, T. Bretheau and P. Gilormini [Eds.], Homogeneisation en Mecanique des Materiaux, Hermes Science Publication, 2001.

45. I. Doghri, C. Friebel, *Effective elasto-plastic properties of inclusion-reinforced composites. Study of shape, orientation and cyclic response*, Mechanics of Materials, **37**, 45–68, 2005.